

Beyond Levermore-Pomraning for Implicit Monte Carlo Radiative Transfer in Binary Stochastic Media

Patrick S. Brantley, N. A. Gentile, George B. Zimmerman

Lawrence Livermore National Laboratory, P.O. Box 808, Livermore, CA 94551
brantley1@llnl.gov, gentile1@llnl.gov, zimmerman3@llnl.gov

Abstract - This paper describes the modifications to the implicit Monte Carlo algorithm for thermal radiative transfer required to implement the Levermore-Pomraning algorithm and a local realization preserving algorithm for transport in participating binary stochastic media. We also describe the approach for incorporating the Su-Pomraning modified closure into both stochastic medium transport algorithms. We assess the accuracy of the various stochastic medium transport algorithms using a thermal radiative transfer binary stochastic medium benchmark suite. The local realization preserving algorithm with the Su-Pomraning modified closure is the most accurate model overall for this benchmark suite.

I. INTRODUCTION

In a stochastic medium, the material properties at a given spatial location are known only statistically [1]. The most common approach to solving particle transport problems involving binary stochastic media is to use the atomic mix (AM) approximation [1] in which the transport problem is solved using ensemble-averaged (homogenized) material properties. The AM approximation is conceptually simple and computationally efficient but may not be accurate enough for a given application depending on the details of the stochastic material properties. Particle transport through binary stochastic mixtures has received significant research attention in the previous three decades [1, 2]. Much of the research has focused on the development and analysis of approximate deterministic models for the solution of such particle transport problems.

A common approximate model developed initially for solving linear particle transport problems in non-participating binary stochastic media is the Levermore-Pomraning (LP) model [1, 2]. The LP model consists of a coupled system of transport equations for the two materials in the problem. The LP model is exact for purely absorbing non-participating media. The accuracy of the LP model for problems with scattering has previously been studied numerically with deterministic solution approaches by Adams, Larsen, and Pomraning [3] using a suite of benchmark problems involving a non-stochastic isotropic angular flux incident on one boundary of a one-dimensional planar geometry binary stochastic medium. These benchmark comparisons demonstrated that the LP model produces qualitatively correct and semi-quantitatively correct results for the reflection and transmission values.

Zimmerman and Adams [4] first proposed a Monte Carlo algorithm that is numerically equivalent to the LP approximation and another Monte Carlo algorithm that should possess increased accuracy as a result of improved local material realization preservation. Zimmerman and Adams [4] numerically demonstrated that the base Monte Carlo LP algorithm solves the Levermore-Pomraning equations and that the improved local realization preserving (LRP) algorithm is generally more accurate by comparing the results of these algorithms to the standard suite of planar geometry incident angular flux binary stochastic mixture benchmark transport solutions [3]. Brantley [5] extended the benchmark comparisons of Zimmerman

and Adams to include the material scalar flux distributions as well as to interior source problems.

Thermal radiative transfer problems are characterized by a radiation field tightly coupled to a participating material energy field. Radiative transfer through a stochastic medium can occur, for example, in inertial confinement fusion targets in which hydrodynamic instabilities at material interfaces can produce a turbulent (stochastic) medium. These types of applications were the original motivation for the seminal work by Levermore et al. [2], although much of the subsequent research has addressed linear particle transport problems in a non-participating medium. Miller [6] and Miller et al. [7] first investigated the solution of binary stochastic medium radiative transfer problems with a participating medium. They generated benchmark ensemble-averaged results for a particular binary stochastic medium radiative transfer problem and compared the accuracy of the atomic mix approximation, an adaptation of the standard deterministic LP model to radiative transfer with participating media, and an adaptation of a deterministic model due to Su and Pomraning [8] that attempts to incorporate the effects of scattering in the statistical coupling terms arising in the LP model. For the binary stochastic medium benchmark problem examined, the AM approximation generally under-predicts transmission of radiation whereas the LP approximation generally over-predicts transmission. The Su-Pomraning extension of the LP model (which we refer to as LP-SP) exhibits accuracy improvements over the LP model for the problems examined by Miller et al. [7].

The implicit Monte Carlo (IMC) algorithm [9] is the standard Monte Carlo algorithm for modeling time-dependent thermal radiative transfer problems with a participating medium. Brantley, Gentile, and Zimmerman [10] previously described the extensions to the IMC algorithm required to incorporate the Monte Carlo LP algorithm (LP). In this work, we describe the further extensions to the IMC algorithm required to incorporate the improved local realization preserving algorithm (LRP) originally proposed by Zimmerman and Adams [4] for the solution of linear particle transport problems in binary stochastic media. We also present IMC solutions incorporating the Su-Pomraning modified closure into the LP (LP-SP) and LRP (LRP-SP) IMC algorithms. We compare the accuracy of the atomic mix, LP, LP-SP, LRP, and LRP-SP approximations

for thermal radiative transfer problems using the benchmark suite of Miller et al. [7].

The remainder of this paper is organized as follows. We describe the radiative transfer problem under investigation and the modifications to the standard implicit Monte Carlo algorithm required to incorporate algorithms for binary stochastic media in Section II. We then present numerical results from benchmark problems to assess the accuracy of the proposed algorithms in Section III. We conclude with a discussion and suggestions for future work in Section IV.

II. IMC ALGORITHMS FOR BINARY STOCHASTIC MEDIA

We consider thermal photon transport in a binary stochastic medium described by temporally-stationary and spatially-homogeneous isotropic Markovian statistics. In the absence of physical scattering and external sources, the grey radiative transfer equations for material i , with $i = 0, 1$ and $i \neq j$, are given by [1, 7]

$$\frac{1}{c} \frac{\partial I_i}{\partial t} + \underline{\Omega} \cdot \underline{\nabla} I_i + \sigma_{a,i} I_i = \frac{1}{4\pi} \sigma_{a,i} c u_{r,i} + \Theta \left[\frac{1}{\Lambda_j} I_j - \frac{1}{\Lambda_i} I_i \right], \quad (1a)$$

$$\frac{\partial u_{m,i}}{\partial t} = \sigma_{a,i} \int_{4\pi} I_i d^2\Omega - \sigma_{a,i} c u_{r,i}. \quad (1b)$$

Here $\underline{\Omega}$ is the direction of photon travel, t is the time, c is the speed of light, $\sigma_{a,i}$ is the absorption opacity for material i , and Λ_i is the mean chord length (mean slab width in one-dimensional planar geometry) in material i . $I_i(\underline{r}, \underline{\Omega}, t)$ is the intensity of radiation at position \underline{r} traveling in direction $\underline{\Omega}$ at time t conditioned on material i being present at position \underline{r} and time t . $u_{r,i} = aT_i^4$ is the equilibrium radiation energy density in material i , where a is the radiation energy density constant and T_i is the temperature in material i , and $u_{m,i}$ is the material energy density in material i . The last two terms on the right side of Eq. (1a) arise from the Levermore-Pomraning closure for stochastic medium transport and couple materials i and j . The term $\frac{1}{\Lambda_i} I_i$ can be interpreted as the rate per unit volume at which photons at position \underline{r} and moving in direction $\underline{\Omega}$ exit material i and enter material j ; $\frac{1}{\Lambda_j} I_j$ can then be interpreted as a probability per unit path length that a photon in material i enters material j . The other coupling term has an analogous interpretation and represents a source of photons entering material i from material j . The parameter Θ in Eq. (1a) is a general multiplier on the Markovian transition functions that can be used to implement modified closure models. Setting the multiplier $\Theta = 1$ in Eq. (1a) produces the standard LP model. Eq. (1b) is a material energy balance equation for material i .

The implicit Monte Carlo equations [9] for material i of a binary stochastic medium including the Levermore-Pomraning closure for the coupling of the materials [2, 7, 10] are given by:

$$\begin{aligned} \frac{1}{c} \frac{\partial I_i}{\partial t} + \underline{\Omega} \cdot \underline{\nabla} I_i + \sigma_{a,i} I_i &= \frac{1}{4\pi} \sigma_{a,i}^n (1 - f_i^n) \int_{4\pi} I_i d^2\Omega' \\ &+ \frac{1}{4\pi} \sigma_{a,i}^n f_i^n c u_{r,i}^n + \Theta^n \left[\frac{1}{\Lambda_j} I_j - \frac{1}{\Lambda_i} I_i \right], \end{aligned} \quad (2a)$$

$$u_{m,i}^{n+1} = u_{m,i}^n + \sigma_{a,i}^n f_i^n \int_{\tau^n}^{\tau^{n+1}} \int_{4\pi} I_i d^2\Omega dt - \sigma_{a,i}^n f_i^n \Delta t^n c u_{r,i}^n. \quad (2b)$$

Here a superscript n denotes a quantity evaluated at the beginning of the time step. The quantity

$$f_i^n = \frac{1}{1 + \beta_i^n c \sigma_{a,i}^n \Delta t^n}, \quad (3)$$

is the ‘‘Fleck factor’’ in material i that serves to model a portion of the absorption and subsequent reemission of photons within a time step Δt^n as effective isotropic scattering, where

$$\beta_i = \frac{\partial u_{r,i}}{\partial u_{m,i}}. \quad (4)$$

Setting the multiplier $\Theta^n = 1$ in Eq. (2a) produces the standard LP model.

1. Su-Pomraning (SP) Closure

The correlation length, Λ_c , for a binary stochastic medium with material indices 0 and 1 is given by [1]

$$\frac{1}{\Lambda_c} = \frac{1}{\Lambda_0} + \frac{1}{\Lambda_1}. \quad (5)$$

A small correlation length therefore implies that the mean slab width for one or both materials is small. Su and Pomraning [8] derived a closure multiplier Θ_{SP} by considering the small correlation length limit and requiring the LP model with the modified closure to give the correct exponential decay for a source-free halfline albedo linear transport problem in rod geometry. Miller et al. [7] applied the modified closure of Su and Pomraning to the deterministic solution of time-dependent thermal radiative transfer problems in participating binary stochastic media and found consistent improvement in accuracy over the LP model. Brantley [11] described how to incorporate the Su-Pomraning closure multiplier into linear Monte Carlo particle transport algorithms for binary stochastic media. Brantley [12] subsequently demonstrated that the Levermore-Pomraning model with the Su-Pomraning closure asymptotically limits to the correct diffusion equation with atomically-mixed material properties for linear transport problems in a certain asymptotic limit.

Defining an ‘‘effective scattering’’ opacity as

$$\sigma_{s,eff,i}^n = \sigma_{a,i}^n (1 - f_i^n), \quad (6)$$

an ‘‘effective absorption’’ opacity as

$$\sigma_{a,eff,i}^n = f_i^n \sigma_{a,i}^n, \quad (7)$$

and the total opacity as

$$\sigma_{t,i}^n = \sigma_{a,eff,i}^n + \sigma_{s,eff,i}^n = \sigma_{a,i}^n, \quad (8)$$

we can rewrite Eq. (2a) as

$$\frac{1}{c} \frac{\partial I_i}{\partial t} + \underline{\Omega} \cdot \underline{\nabla} I_i + \sigma_{t,i}^n I_i = \frac{1}{4\pi} \sigma_{s,eff,i}^n \int_{4\pi} I_i d^2\Omega'$$

$$+ \frac{1}{4\pi} \sigma_{a,eff,i}^n c u_{r,i}^n + \Theta^n \left[\frac{1}{\Lambda_j} I_j - \frac{1}{\Lambda_i} I_i \right]. \quad (9)$$

For the IMC equations as written in Eq. (9), we can compute the Su-Pomraning closure multiplier as

$$\Theta_{SP}^n = \frac{\sqrt{\langle \sigma_{a,eff}^n \rangle \langle \sigma_t^n \rangle \left[\langle \sigma_{a,eff}^n \rangle (\sigma_{t,1}^n - \sigma_{t,0}^n)^2 + \langle \sigma_t^n \rangle (\sigma_{a,eff,1}^n - \sigma_{a,eff,0}^n)^2 \right]}}{\left[\langle \sigma_{a,eff}^n \rangle (\sigma_{t,1}^n - \sigma_{t,0}^n) \right]^2 + \left[\langle \sigma_t^n \rangle (\sigma_{a,eff,1}^n - \sigma_{a,eff,0}^n) \right]^2}, \quad (10)$$

where the ensemble-averaged opacity values are computed using the material probabilities $p_i = \Lambda_i / (\Lambda_0 + \Lambda_1)$ as $\langle \sigma_x^n \rangle = p_0 \sigma_{x,0}^n + p_1 \sigma_{x,1}^n$. Setting $\Theta^n = \Theta_{SP}^n$ in Eq. (9) produces the LP-SP model.

2. Implicit Monte Carlo Algorithm Modifications

Much of the standard implicit Monte Carlo algorithm using the atomic mix approximation is unaltered by the introduction of algorithms to model radiative transfer through a stochastic medium. A Monte Carlo photon must maintain an additional identifier describing the material in which the photon is currently located. This material identifier must be appropriately sampled (in proportion to the material probability) when a photon is created from a source or enters the problem via an external boundary. The IMC equations are solved using a spatial mesh with Monte Carlo photons advanced over time steps. In addition to the standard distance to collision, distance to zone boundary, and distance to census values that must be sampled or computed [9], a new event, the distance to material interface, $d_{interface}$, is sampled from the appropriate distribution characterizing the chord lengths in the material. Assuming Markovian statistics and accounting for the closure multiplier, a distance to material interface in material i , λ_i , is sampled from the exponential distribution

$$f_i(\lambda_i) = \frac{\Theta^n}{\Lambda_i} \exp\left(-\frac{\Theta^n}{\Lambda_i} \lambda_i\right), \quad (11)$$

resulting in

$$d_{interface} = -\frac{\Lambda_i}{\Theta^n} \ln(\xi), \quad (12)$$

where ξ is a random number. The sampling of a distance to material interface value essentially treats the $\frac{\Theta^n}{\Lambda_i} I_i$ on the right side of Eq. (9). For the specific case of one-dimensional planar geometry, a distance to material interface is obtained by sampling a material slab width from the exponential distribution given by Eq. (11) and dividing by the magnitude of the photon direction cosine, $|\mu|$, to account for the direction of photon motion, i.e.,

$$d_{interface} = -\frac{\Lambda_i}{|\mu| \Theta^n} \ln(\xi), \quad (13)$$

where ξ is a random number.

If the distance to material interface event is selected, the Monte Carlo photon is moved to the material interface location and the material identifier changed to the opposite material. An important aspect of the algorithm in a stochastic medium is to keep the Monte Carlo photon in the same material when a zone boundary is crossed to preserve the sampled local material realization. (This portion of the algorithm must be

modified to account for spatially inhomogeneous material statistics if present.) In addition, photons retrieved from census at the beginning of the time step should remain in the same material in which they were placed into census at the end of the previous time step to avoid a dependence of the results on the time step. (This portion of the algorithm must be modified to account for temporally non-stationary material statistics if present.) Finally, a material energy balance equation for each material is required.

The LP and LRP implicit Monte Carlo algorithms differ in how they treat the distance to material interface values. The IMC LP algorithm resamples a new distance to material interface in the direction of photon travel, $d_{interface}$, after every event – census, effective scattering, material interface crossing, and zone boundary crossing. As a result, a photon encounters a different material realization following an effective scatter which is nonphysical. We therefore expect the IMC LP algorithm to be least accurate in materials with significant effective scattering ($f_i \rightarrow 0$ implying strongly absorbing materials) and optically-thick mean chord lengths.

In contrast, the IMC LRP algorithm samples distance to material interface values in the forward and backward directions of photon travel, $d_{interface}^+$ and $d_{interface}^-$, respectively. When a photon is moved, these distance to material interface values are evolved appropriately. In one-dimensional planar geometry, the distance to material interface values in the forward and backward directions are adjusted to account for the change in direction of flight of the photon after a sampled effective scattering. The forward and backward distance to material interface values are switched if the photon is backscattered (i.e., the value of the direction cosine μ changes sign in one-dimensional planar geometry or using a probabilistic model in multiple dimensions). If $d_{interface}^+$ is the minimum distance, the photon is moved to the material interface, the material identifier is switched, a new $d_{interface}^+$ value is sampled, and $d_{interface}^-$ is set to zero. In the IMC LRP algorithm, a photon can move, undergo effective scatters, and cross zone boundaries within one material and encounter the same local material realization, which is physically more realistic than the LP algorithm. As a result, we expect the IMC LRP algorithm to be more accurate than the LP algorithm. The IMC LRP algorithm remains approximate if a photon reenters the same material at the same location within one history, as the sampled material realization will be different upon reentry.

III. NUMERICAL RESULTS

We implemented the IMC LP, LRP, LP-SP, and LRP-SP algorithms in an experimental version of the LLNL Kull IMC package [13]. This IMC package already possessed multiple material infrastructure that significantly facilitated the implementation of the modifications required to enable the stochastic medium algorithms. The implementation of the stochastic medium transport algorithms is general (multiple spatial dimensions, multigroup opacities, parallelism via domain decomposition and replication), although testing of the capability to this point has been limited to one-dimensional planar geometry grey radiative transfer problems.

1. Linear Transport Benchmark Suite

We simulated the binary stochastic medium linear particle transport benchmark suite of Adams et al. [3] as an initial test of the implemented IMC capabilities. This time-independent one-dimensional planar geometry incident angular flux benchmark suite includes three material mean chord length combinations and three material scattering ratio combinations (nine total material cases). The material parameters for the benchmark transport problems are given in Table II in the Appendix, where the scattering ratio for material i is defined as $c_i = \sigma_{s,i}/\sigma_{t,i}$ and $\sigma_{s,i}$ and $\sigma_{t,i}$ are the scattering and total cross sections for material i , respectively. The different case numbers (i.e., 1, 2, and 3) represent permutations of materials with mean material slab widths of optical depth 0.1, 1.0, and 10.0. The different case letters (i.e., a, b, and c) represent varying amounts of scattering for each material. For each set of material parameters (cases 1, 2, and 3), three sets of scattering ratio combinations (cases a, b, and c) are considered. We focus here on a spatial domain size of 10 cm. To solve these linear transport problems with the IMC implementation, we used a large specific heat capacity to decouple the transport from the material. We performed the IMC simulations with 10^5 Monte Carlo photons per time step, one hundred uniformly-spaced zones, and 100 time steps of 5×10^{-9} s.

The cumulative ensemble-averaged reflection and transmission values from our IMC simulations are shown in Tables III and IV, respectively, in the Appendix. For the cases simulated, the reflection and transmission values from our IMC simulations agree with previous independent Monte Carlo LP and LRP results [5] and Monte Carlo LP-SP results [11] and unpublished LRP-SP results to typically three to four digits (significantly better than 1%). These Monte Carlo results agree with the deterministic S_{16} LP results in [3] and the deterministic LP-SP results in [8] to typically two to three digits. Improved agreement between the Monte Carlo and deterministic results may be obtained if the deterministic results were generated using higher angular quadrature orders. These numerical results demonstrate that the basic Monte Carlo LP, LRP, LP-SP, and LRP-SP implementations in the IMC package are correct in the linear transport limit.

2. Radiative Transfer Benchmark Suite

We investigate the accuracy of the various IMC algorithms using the binary stochastic medium radiative transfer benchmark suite of Miller [6] and Miller et al. [7]. This one-dimensional planar geometry benchmark suite consists of a strongly absorbing material 0 ($\sigma_{a,0} = 1000 \text{ cm}^{-1}$) with smaller mean chord length mixed with a more weakly absorbing material 1 ($\sigma_{a,1} = 5 \text{ cm}^{-1}$) with larger mean chord length. The problem spatial domain is given by $0 \leq z \leq L = 0.15 \text{ cm}$. The materials are distributed according to Markovian statistics (exponentially) with the mean chord lengths given in Table I. (We note that the mean chord length values are listed incorrectly in Ref. [7]; the correct values given in Ref. [6] are one order of magnitude smaller.) Problem A represents the most spatial heterogeneity, with the heterogeneity decreasing in the subsequent problems until the atomic mix limit is approached in Problem D. For the specified mean chord lengths,

the probability of material i being present, $p_i = \Lambda_i/(\Lambda_0 + \Lambda_1)$, is constant for all mean chord length cases. As a result, the atomic mix approximation result is the same for all cases. The initial temperature of the materials is $T_{init} = 30 \text{ eV}$, and a cosine-distributed source of radiation at 300 eV is present at $z = 0$. A special form of the specific heat capacity is assumed, $C_{v,i} = \frac{4a}{\rho_i} T_i^3$, where ρ_i is the mass density of material i , which results in a linearization of the material energy balance equation. We simulated this problem using the IMC package with the various stochastic medium models using 5×10^6 Monte Carlo photons per time step, one thousand uniformly-spaced zones, and an initial time step of 10^{-15} s with a maximum time step of 10^{-12} s.

TABLE I. Radiative Transfer Benchmark Suite Material Parameters

Problem	Λ_0	$\sigma_{t,0}\Lambda_0$	Λ_1	$\sigma_{t,1}\Lambda_1$	Λ_c
	[cm]	[-]	[cm]	[-]	[cm]
A	5.0e-3	5.0e+0	5.0e-1	2.5e+0	4.95e-3
B	5.0e-4	5.0e-1	5.0e-2	2.5e-1	4.95e-4
C	5.0e-5	5.0e-2	5.0e-3	2.5e-2	4.95e-5
D	5.0e-6	5.0e-3	5.0e-4	2.5e-3	4.95e-6

For each of Problems A-D in the benchmark suite and each of the stochastic medium transport algorithms, we plot the ensemble-averaged temperature energy density at the outgoing edge ($z = L$) of the spatial domain scaled by the initial temperature. The ensemble-averaged temperature energy density is computed from the material temperatures using [7]

$$\langle aT^4 \rangle = p_0 aT_0^4 + p_1 aT_1^4, \quad (14)$$

where p_i is the probability of material i being present, as described above. The material temperature in the simulation code is zone-centered, so we plot the temperature in the zone closest to the boundary to represent the value at $z = L$. We also plot the ensemble-averaged transmission at the outgoing edge ($z = L$) of the spatial domain scaled by the initial temperature, where the transmission is given by

$$\langle Trans \rangle = \left\langle \int_0^1 \mu I(L, \mu, t) d\mu \right\rangle. \quad (15)$$

The ensemble-averaged transmission is numerically computed by tallying the energy weight of Monte Carlo photons escaping the domain at $z = L$. Although not plotted, the LP IMC results for the exiting ensemble-averaged temperature and transmission agree with deterministic LP results [6, 7].

We plot in Figs. 1(a) and 1(b) the ensemble-averaged temperature energy density and transmission at the outgoing edge ($z = L$) of the spatial domain for each of the stochastic medium transport algorithms for Problem A. For this problem, the atomic mix approximation significantly underpredicts (~30%) the ensemble-averaged material temperature and transmission. The LP approximation is significantly more accurate than the atomic mix approximation, somewhat overpredicting (~10%) the temperature and transmission. The improved material realization preservation of the LRP algorithm results

in improved accuracy (~6-7%) over the LP algorithm. The LP-SP algorithm incorporating the SP closure multiplier is slightly more accurate (~4-6%) than the LRP algorithm. The LRP-SP algorithm that utilizes both improved local material realization preservation and the SP closure modifier is the most accurate (~1%). We observe that the SP closure improves the accuracy for both the LP and LRP algorithms.

~8-10%. The SP closure improves the accuracy of both the LP and LRP algorithms to better than the AM approximation. The LP-SP algorithm overpredicts the temperature and transmission by ~4-6%, while the LRP-SP algorithm overpredicts these quantities by ~2-4%. The IMC algorithms using the SP closure are more accurate than the AM approximation for Problem B.

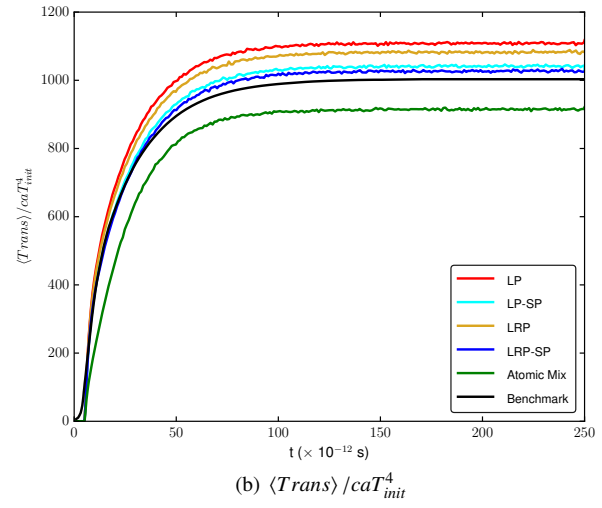
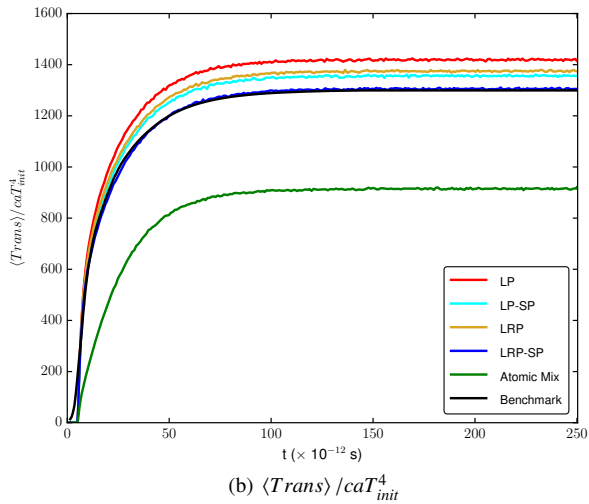
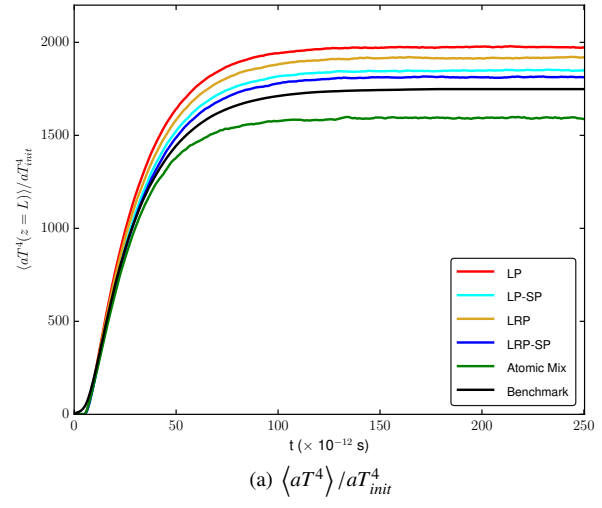
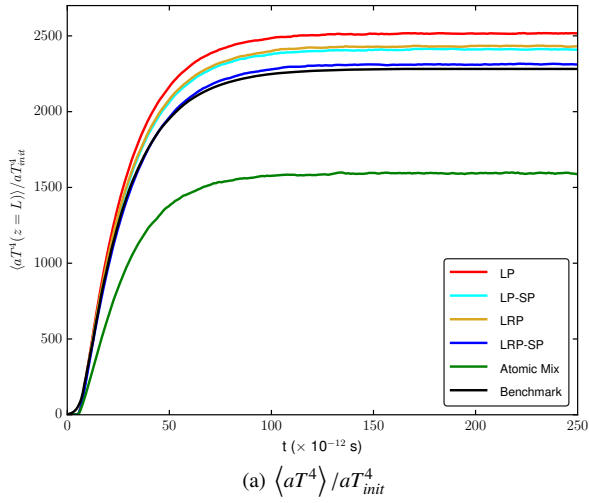


Fig. 1. Problem A ensemble-averaged quantities at $z = L$ versus time ($\times 10^{-12}$ s)

Fig. 2. Problem B ensemble-averaged quantities at $z = L$ versus time ($\times 10^{-12}$ s)

We plot in Figs. 2(a) and 2(b) the ensemble-averaged temperature energy density and transmission at the outgoing edge ($z = L$) of the spatial domain for each of the stochastic medium transport algorithms for Problem B. The AM approximation is more accurate for Problem B but underpredicts the temperature and transmission by ~8-9%. The LP steady state solution is slightly less accurate than AM, overpredicting the temperature and transmission by ~11-13%. The LRP algorithm is of comparable accuracy to the AM approximation with errors of

We plot in Figs. 3(a) and 3(b) the ensemble-averaged temperature energy density and transmission at the outgoing edge ($z = L$) of the spatial domain for each of the stochastic medium transport algorithms for Problem C. The AM approximation is generally accurate (to within ~1%) for Problem C except for larger errors in the transient phase. The LP and LRP algorithms are more accurate than AM in the transient phase and slightly less accurate (errors of ~1-3%) in the steady state. The LP-SP and LRP-SP algorithms using the SP closure are more

accurate (to within ~1%) than the LP and LRP algorithms that do not use the SP closure.

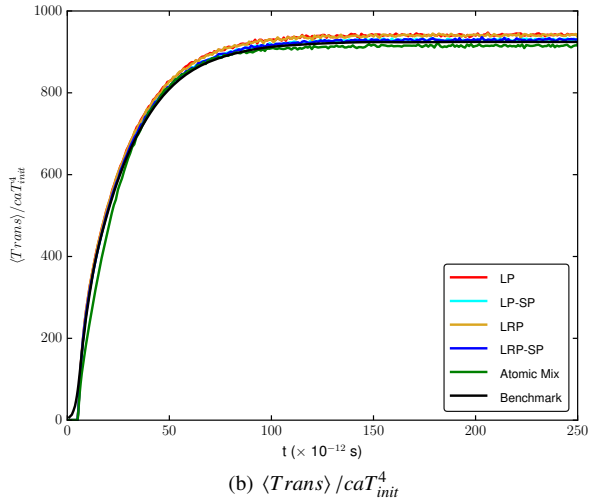
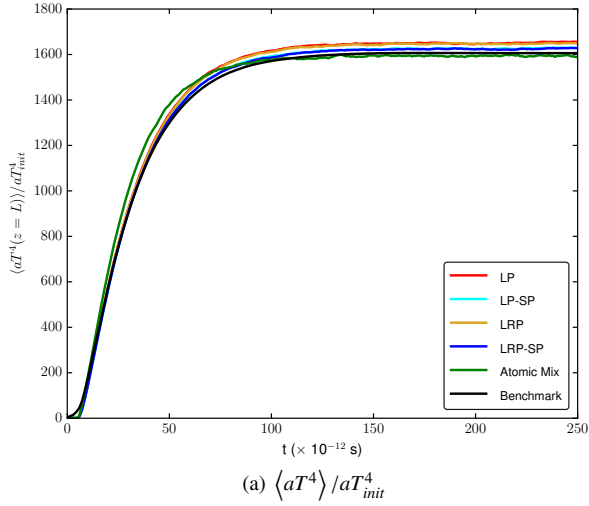


Fig. 3. Problem C ensemble-averaged quantities at $z = L$ versus time ($\times 10^{-12}$ s)

Finally, we plot in Figs. 4(a) and 4(b) the ensemble-averaged temperature energy density and transmission at the outgoing edge ($z = L$) of the spatial domain for each of the stochastic medium transport algorithms for Problem D. The LP, LRP, LP-SP, and LRP-SP algorithms are all accurate to within ~1% for this small mean chord length case. The AM solution limits to the benchmark solution only in the steady state. The discrepancy in the transient temperature and transmission profiles between the AM approximation and the benchmark and other stochastic medium transport algorithm results was previously observed in [6] and [7]. This discrepancy was subsequently investigated using asymptotic analysis in [14] and shown to be related to the absence of material transition terms in the material energy balance equation. We observe that all of

the explicit stochastic medium transport algorithms (LP, LRP, LP-SP, and LRP-SP) limit to the benchmark result in both the transient and steady state phases as the atomic mix limit is approached.

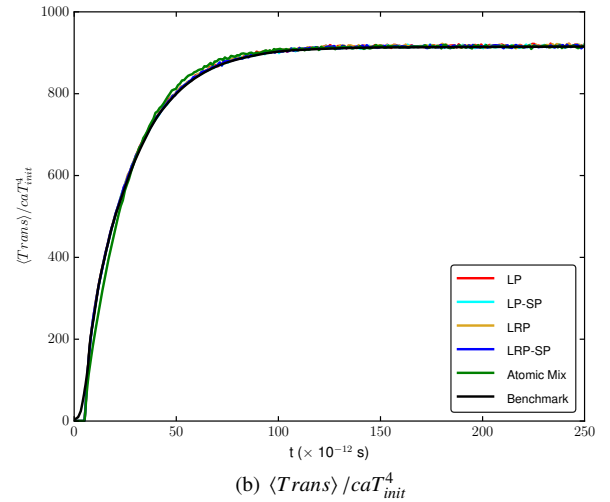
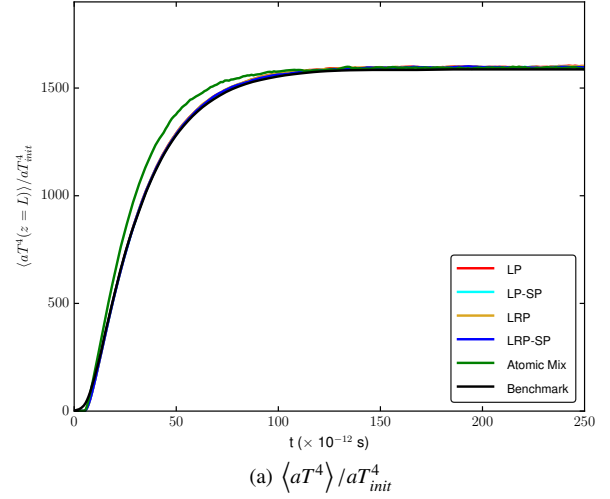


Fig. 4. Problem D ensemble-averaged quantities at $z = L$ versus time ($\times 10^{-12}$ s)

IV. CONCLUSIONS

We described the modifications to the standard implicit Monte Carlo algorithm for thermal radiative transfer necessary to implement multiple approaches for incorporating the effects of binary stochastic media. We have developed both an LP-equivalent algorithm and an improved algorithm that locally preserves the material realization. We have also incorporated the Su-Pomraning modified closure into both the LP and LRP algorithms. The IMC LP and LRP algorithms can be more accurate than the AM algorithm, though not for all test cases examined. The IMC LRP algorithm is generally more accurate

than the LP algorithm. The Su-Pomraning closure improves the accuracy of both the LP and LRP algorithms, with the LRP-SP algorithm being the most accurate algorithm overall.

In future work, we would like to investigate modifications of the stochastic medium algorithms to account for non-homogeneous and non-stationary material statistics. In addition, we would like to extend the benchmark comparisons to include multi-dimensional geometry and multiple frequency groups.

V. ACKNOWLEDGMENTS

This work performed under the auspices of the U.S. Department of Energy by Lawrence Livermore National Laboratory under Contract DE-AC52-07NA27344.

REFERENCES

1. G. C. POMRANING, *Linear Kinetic Theory and Particle Transport in Stochastic Mixtures*, World Scientific Publishing Co. Pte. Ltd., River Edge, New Jersey, USA (1991).
2. C. D. LEVERMORE, G. C. POMRANING, D. L. SANZO, and J. WONG, "Linear Transport Theory in a Random Medium," *J. Math. Phys.*, **27**, 2526–2536 (1986).
3. M. L. ADAMS, E. W. LARSEN, and G. C. POMRANING, "Benchmark Results for Particle Transport in a Binary Markov Statistical Medium," *J. Quant. Spect. Rad. Trans.*, **42**, 253–266 (1989).
4. G. B. ZIMMERMAN and M. L. ADAMS, "Algorithms for Monte-Carlo Particle Transport in Binary Statistical Mixtures," *Trans. Am. Nucl. Soc.*, **64**, 287 (1991).
5. P. S. BRANTLEY, "A Benchmark Comparison of Monte Carlo Particle Transport Algorithms for Binary Stochastic Mixtures," *J. Quant. Spect. Rad. Trans.*, **112**, 599–618 (2011).
6. D. S. MILLER, "Benchmarks and Models for 1-D Radiation Transport in Stochastic Participating Media," *Lawrence Livermore National Laboratory Report UCRL-LR-140199* (2000).
7. D. S. MILLER, F. GRAZIANI, and G. RODRIGUE, "Benchmarks and models for time-dependent grey radiation transport with material temperature in binary stochastic media," *J. Quant. Spect. Rad. Trans.*, **70**, 115 (2001).
8. B. SU and G. C. POMRANING, "Limiting Correlation Length Solutions in Stochastic Radiative Transfer," *J. Quant. Spect. Rad. Trans.*, **51**, 893–912 (1994).
9. J. A. FLECK, JR. and J. D. CUMMINGS, "An Implicit Monte Carlo Scheme for Calculating Time and Frequency Dependent Nonlinear Radiation Transport," *J. Comput. Phys.*, **8**, 313 (1971).
10. P. S. BRANTLEY, N. A. GENTILE, and G. B. ZIMMERMAN, "A Levermore-Pomraning Algorithm for Implicit Monte Carlo Radiative Transfer in Binary Stochastic Media," *Trans. Am. Nucl. Soc.*, **105**, 498 (2011), on CD-ROM.
11. P. S. BRANTLEY, "Incorporation of a Modified Closure in a Monte Carlo Particle Transport Algorithm for Binary Stochastic Media," *Trans. Am. Nucl. Soc.*, **106**, 342–345, on CD-ROM (2012).
12. P. S. BRANTLEY, "Modified Closures in Monte Carlo Algorithms for Diffusive Binary Stochastic Media Transport Problems," *Trans. Am. Nucl. Soc.*, **114**, 369–372, on USB (2016).
13. N. A. GENTILE, N. KEEN, and J. RATHKOPF, "The KULL IMC Package," *Lawrence Livermore National Laboratory Report UCRL-JC-132743* (1998).
14. A. K. PRINJA and G. L. OLSON, "Grey radiative transfer in binary statistical media with material temperature coupling: asymptotic limits," *J. Quant. Spect. Rad. Trans.*, **90**, 131–159 (2005).

APPENDIX: LINEAR TRANSPORT BENCHMARK SUITE MATERIAL PARAMETERS AND NUMERICAL RESULTS

TABLE II. Linear Transport Benchmark Suite Material Parameters

Case	$\sigma_{t,0}$	Λ_0	$\sigma_{t,1}$	Λ_1	Case	c_0	c_1
1	10/99	99/100	100/11	11/100	a	0.0	1.0
2	10/99	99/10	100/11	11/10	b	1.0	0.0
3	2/101	101/20	200/101	101/20	c	0.9	0.9

TABLE III. Linear Transport Benchmark Suite Reflection Results

Case	Case	MC				IMC			
		LP [5]	LRP [5]	LP-SP [11]	LRP-SP	LP	LRP	LP-SP	LRP-SP
1	a	0.3782	0.4009	0.4489	0.4558	0.3780	0.4009	0.4487	0.4556
	b	0.0586	0.0776	0.0588	0.0778	0.0586	0.0775	0.0587	0.0777
	c	0.3695	0.4069	0.4014	0.4218	0.3695	0.4067	0.4012	0.4216
2	a	0.1805	0.2224	0.2784	0.3194	0.1803	0.2224	0.2782	0.3192
	b	0.2183	0.2854	0.2187	0.2858	0.2181	0.2852	0.2185	0.2856
	c	0.2896	0.4009	0.2890	0.3996	0.2893	0.4006	0.2888	0.3994
3	a	0.6076	0.6542	0.7242	0.7414	0.6073	0.6537	0.7239	0.7408
	b	0.0240	0.0360	0.0240	0.0360	0.0239	0.0359	0.0239	0.0359
	c	0.3261	0.3990	0.3488	0.4097	0.3259	0.3988	0.3486	0.4094

TABLE IV. Linear Transport Benchmark Suite Transmission Results

Case	Case	MC				IMC			
		LP [5]	LRP [5]	LP-SP [11]	LRP-SP	LP	LRP	LP-SP	LRP-SP
1	a	0.0264	0.0220	0.0107	0.0101	0.0264	0.0220	0.0107	0.0101
	b	0.0015	0.0016	0.0016	0.0017	0.0015	0.0016	0.0016	0.0017
	c	0.0238	0.0209	0.0140	0.0126	0.0238	0.0209	0.0140	0.0126
2	a	0.1284	0.1060	0.0670	0.0521	0.1283	0.1058	0.0669	0.0520
	b	0.1794	0.1953	0.1800	0.1959	0.1791	0.1949	0.1797	0.1956
	c	0.1950	0.1956	0.1330	0.1297	0.1948	0.1952	0.1329	0.1295
3	a	0.2404	0.1980	0.1241	0.1098	0.2398	0.1975	0.1237	0.1096
	b	0.0757	0.0765	0.0757	0.0765	0.0756	0.0763	0.0756	0.0763
	c	0.1197	0.1180	0.0658	0.0633	0.1195	0.1177	0.0657	0.0633